

# The Molecular Chaperone HSP70 Binds to and Stabilizes NOD2, an Important Protein Involved in Crohn Disease\*

Received for publication, February 18, 2014, and in revised form, April 25, 2014. Published, JBC Papers in Press, April 30, 2014, DOI 10.1074/jbc.M114.557686

Vishnu Mohanan<sup>†</sup> and Catherine Leimkuhler Grimes<sup>†S1</sup>

From the Departments of <sup>†</sup>Biological Sciences and <sup>S</sup>Chemistry and Biochemistry, University of Delaware, Newark, Delaware 19716

**Background:** NOD2, an innate immune receptor, senses bacterial cell wall fragments. NOD2 mutations are linked to Crohn disease.

**Results:** HSP70 enhances NOD2's activity and increases its half-life.

**Conclusion:** NOD2 mutants are less stable than the wild type. HSP70 overexpression stabilizes the NOD2 Crohn mutants and rescues its activity.

**Significance:** Stabilization of the NOD2 mutants may provide an effective therapy for Crohn disease.

Microbes are detected by the pathogen-associated molecular patterns through specific host pattern recognition receptors. Nucleotide-binding oligomerization domain-containing protein 2 (NOD2) is an intracellular pattern recognition receptor that recognizes fragments of the bacterial cell wall. NOD2 is important to human biology; when it is mutated it loses the ability to respond properly to bacterial cell wall fragments. To determine the mechanisms of misactivation in the NOD2 Crohn mutants, we developed a cell-based system to screen for protein-protein interactors of NOD2. We identified heat shock protein 70 (HSP70) as a protein interactor of both wild type and Crohn mutant NOD2. HSP70 has previously been linked to inflammation, especially in the regulation of anti-inflammatory molecules. Induced HSP70 expression in cells increased the response of NOD2 to bacterial cell wall fragments. In addition, an HSP70 inhibitor, KNK437, was capable of decreasing NOD2-mediated NF- $\kappa$ B activation in response to bacterial cell wall stimulation. We found HSP70 to regulate the half-life of NOD2, as increasing the HSP70 level in cells increased the half-life of NOD2, and down-regulating HSP70 decreased the half-life of NOD2. The expression levels of the Crohn-associated NOD2 variants were less compared with wild type. The overexpression of HSP70 significantly increased NOD2 levels as well as the signaling capacity of the mutants. Thus, our study shows that restoring the stability of the NOD2 Crohn mutants is sufficient for rescuing the ability of these mutations to signal the presence of a bacterial cell wall ligand.

The human innate immune system is charged with a tremendous task, *i.e.* to provide the first line of defense against invading pathogens. This task is even more challenging in the human gut where over a trillion commensal bacteria reside. Thus, this ancient system must overlook the signal from the “good” bacteria while properly responding to the “bad” bacteria (1–3). To accomplish this daunting task, the system relies partially on a

complex system of receptors known collectively as innate immune receptors or pattern recognition receptors (4). These receptors are made up of both Toll-like receptors (TLRs)<sup>2</sup> and Nod-like receptors (5–8). It has recently been shown that these families of receptors work together to form an intricate set of feedback loops to ensure that the innate immune system properly responds to pathogenic and commensal bacteria (9, 10). One can imagine the consequences if there is a breakdown of one of the receptors. NOD2 (nucleotide-binding oligomerization domain-containing protein 2) has been shown to be mutated in Crohn disease, a gastrointestinal disorder affecting the upper intestines (11). Inohara and co-workers (12) have shown that the Crohn mutants of NOD2 do not properly respond to their corresponding bacterial signals. More than 58 mutations in the *NOD2* gene have been linked with various diseases, and 80% of these mutations are reported to be linked with Crohn disease (13). The three highest point mutations with an association, R702W, G908R, and 1007fs, represent 32, 18, and 31%, respectively, of the total Crohn disease mutations (14). Normally, NOD2 participates in the innate immune response by sensing fragments of bacterial peptidoglycan (15). The human protein, NOD2, is found in peripheral blood mononuclear cells such as macrophages, granulocytes, dendritic cells, and along the intestinal epithelial cells (15–17). It has been shown that NOD2 binds to muramyl dipeptide (MDP), a small degradation fragment of the bacterial cell wall (18, 19). Upon binding to its bacterial cell wall fragment, NOD2 interacts with RIP2 to activate the canonical NF- $\kappa$ B pathway, triggering an inflammatory response (20). The Crohn-associated NOD2 mutants show a reduction in NF- $\kappa$ B signaling (12). NOD2 has a tri-domain structure consisting of two N-terminal caspase recruitment domains, a nucleotide binding domain, and a C-terminal leucine-rich repeat (21). Mutations in the LRR region of NOD2 have been shown to increase the incidence of Crohn disease (11, 22).

Given the importance of NOD2 to human inflammatory disorders, there has been an urgency to understand the proper

\* This work was supported, in whole or in part, by National Institutes of Health Grant P20GM103541 from NIGMS.

<sup>†</sup> To whom correspondence should be addressed: Dept. of Chemistry and Biochemistry, University of Delaware, Newark, DE 19716. Tel.: 302-831-2985; Fax: 302-831-6335; E-mail: cgrimes@udel.edu.

<sup>2</sup> The abbreviations used are: TLR, Toll-like receptor; HSP70, heat shock protein 70; HSP90, heat shock protein 90; GGA, geranylgeranylacetone; MDP, muramyl dipeptide; dox, doxycycline; co-IP, co-immunoprecipitation.

## HSP70 Regulates the Stability of NOD2

signaling mechanism of NOD2 in the innate immune response. With the proper signaling cascade understood, treatments for Crohn disease can be developed. Recently, three independent studies have shed light on the control mechanisms of NOD2 signaling. First, Nunez and co-workers (23) demonstrated that NOD2 is negatively regulated by the protein Erbin. Erbin was shown to directly interact with NOD2, and its overexpression inhibited the ability of NOD2 to signal the presence of bacterial cell wall fragments (23). Elegant work by Kobayashi and co-workers (24) went on to show that NOD2 activation via MDP is regulated by proteasomal degradation. Before stimulation, NOD2 forms a complex with heat shock protein 90 (HSP90). Upon binding MDP, NOD2 and HSP90 dissociate. Subsequently, NOD2 undergoes proteasomal degradation (24). This unique mechanism allows NOD2 to tolerate a large influx of MDP and avoid septic shock. In a subsequent study, McDonald and co-workers (25) have shown that NOD2 is negatively regulated by the nucleotide synthesis enzyme carbamoyl-phosphate synthetase/aspartate transcarbamylase/dehydroorotase. Carbamoyl-phosphate synthetase/aspartate transcarbamylase/dehydroorotase was identified as a NOD2-interacting protein and was shown to inhibit the ability of NOD2 to signal the presence of bacterial cell wall ligands. Inhibition of carbamoyl-phosphate synthetase/aspartate transcarbamylase/dehydroorotase increased both the wild type and Crohn-associated NOD2 variants' ability to signal the presence of bacterial cell wall ligands (25). Finally, independent genome-wide siRNA screens identified positive and negative regulators of the NOD2 or NF- $\kappa$ B pathways (26, 27).

In general, two different approaches have been used to identify protein-protein interactors involved in the NOD2-signaling cascade: 1) immunoprecipitation (IP) followed by mass spectrometry and 2) siRNA screens (25, 27). Both approaches have been successful in identifying new protein-protein interactors of NOD2. However, the mechanism for rescuing the Crohn phenotype remains unresolved. To determine novel protein-protein interactors of NOD2, we designed a cell-based system that would allow for identification of interactors that used normal endogenous NOD2 levels in the cell and would allow for essential proteins to be identified. We were intrigued by the tetracycline-inducible promoter system that was developed by Blau and co-workers (28) and has successfully elucidated many signaling mechanisms (29). Tetracycline-regulated expression enabled purification and functional analysis of recombinant connexin channels from mammalian cells (30). We envisioned that this sophisticated system would give us a method to control the expression of an epitope-tagged version of NOD2 in human cells.

Using the tetracycline-regulated expression system, we have identified heat shock protein 70 (HSP70) as a *bona fide* interactor of NOD2. We show that HSP70 increases the half-life of both wild type and the Crohn mutant, NOD2. More importantly, we demonstrate that overexpression of HSP70 is able to rescue the Crohn mutant response to MDP, the bacterial cell wall fragment recognized by NOD2. Our data suggest that the Crohn mutants are inherently unstable and unable to properly respond to the bacterial cell wall ligands. Thus, a novel therapy

providing stability to Crohn disease-associated NOD2 variants could be extremely useful.

## EXPERIMENTAL PROCEDURES

**Cell Culture**—All cell lines used were obtained from American Type Culture Collection (ATCC, Manassas, VA). Phoenix-E cells were used for the generation of retroviruses. We used three cell lines as follows: 1) HEK293T, a human embryonic kidney cell line; 2) HCT 116, a human colon epithelial cell line; and 3) THP-1, a human monocyte cell line. All cell lines were cultured in DMEM, 10% FBS (Atlantic Biologicals), 2 mM L-glutamine, penicillin/streptomycin and grown in a humidified incubator at 37 °C and 5% CO<sub>2</sub>.

**Construction of Tetracycline-regulated NOD2-expressing Stable Cell Lines**—Stable cell lines of HCT 116 and HEK293T cells that express tetracycline-inducible NOD2Myc under the control of RetroTET-ART system were created by viral infection with HRSp-NOD2Myc, transactivator (RTAb), and transrepressor (RTRg) as described previously (28, 31). Phoenix-E cells were used for the generation of retroviruses (32).

**Antibodies and Compounds**—Mouse monoclonal anti-Myc, rabbit monoclonal anti-Myc, rabbit monoclonal anti-HSP70, rat anti-HSP70, mouse monoclonal anti- $\beta$ -actin, mouse monoclonal anti-laminin, and rabbit anti-RIP2 antibody were purchased from Cell Signaling Technology. Mouse monoclonal anti-HSP70 was purchased from Invitrogen. Alexa Fluor-594 goat anti-mouse and Alexa Fluor-488 goat anti-rabbit (Jackson ImmunoResearch) were used as secondary antibodies. Anti-mouse and anti-rabbit IgG HRP-linked secondary antibodies (Cell Signaling Technology) were used for immunoblot. Rabbit NOD2 antiserum, HM2559, was kindly provided by the Podolsky laboratory (33). MDP (Bachem) for stimulating the cells was used at a concentration of 2  $\mu$ M. TNF $\alpha$  (Roche Diagnostics) for stimulating the cells was used at a concentration of 200 nM. HSP70 inhibitor KNK437 was obtained from Calbiochem. HSP70 inducer geranylgeranylacetone (GGA) was obtained from Sigma. Translational inhibitor cycloheximide was obtained from Sigma.

**Co-immunoprecipitation**—Cells were rinsed with 1 $\times$  PBS, and the lysates were collected using freshly prepared lysis buffer (1% Triton X-100, 2 mM EDTA, 4 mM Na<sub>3</sub>PO<sub>4</sub>, 100 mM NaCl, 10 mM MES, pH 5.8, 10 mM NaF, 1 protease inhibitor mixture tablet (Roche Diagnostics)) and lysed by passing through a 21-gauge needle. 4  $\mu$ g of lysates were mixed with the appropriate amount of antibody and incubated for 2 h in the cold. Lysate/antibody mixture was incubated with 40  $\mu$ l of protein A Dynabeads (Invitrogen) (prewashed in PBS and lysis buffer) for 3 h in the cold. After 3 h, lysate/antibody bead mixture was washed four times using 200  $\mu$ l of lysis buffer containing varying concentrations of NaCl as follows: wash 1, 100 mM NaCl; wash 2, 300 mM NaCl; wash 3, 500 mM NaCl; wash 4, 100 mM NaCl. To elute the proteins, two different methods were implemented depending on the downstream analysis as follows. 1) For Western blot analysis, proteins were eluted at 60 °C for 30 min with 2 $\times$  reaction buffer (100 mM Tris-HCl, pH 6.8, 4% SDS, 12% glycerol, 0.008% bromphenol blue, 2%  $\beta$ -mercaptoethanol). 2) For mass spectrometry analysis, proteins were eluted with 5  $\mu$ g/ml of Myc peptide (Sigma) in Tris-buffered saline

(TBS) for 12 h at 4 °C. All eluates were analyzed by running in 7.5% polyacrylamide gels containing 0.1% SDS, followed by immunoblotting or staining using SYPRO® Ruby Protein Gel Stain according to the manufacturer's instruction (Invitrogen). The immunoblot and mass spectrometry analysis procedures are described below.

**Mass Spectrometry Screen**—Samples were subjected to reduction/alkylation with dithiothreitol (Bio-Rad) and iodoacetamide (Sigma). Enzymatic digestion was performed with trypsin (Promega) at 37 °C. Subsequently, samples were desalted and concentrated using Ziptips (Millipore) and applied to target plates with  $\alpha$ -cyano-4-hydroxycinnamic acid matrix (Sigma). Data were collected on a 4800 MALDI-TOF analyzer (ABSciex) in positive ion reflector mode over a mass range of 850–4000 Da, with internal calibration. Select peaks were further analyzed by MS-MS at 1 kV with default calibration. Combined MS and MS-MS data were submitted to Mascot (Matrix Science) and searched against NCBI, with trypsin specificity, 100 ppm mass tolerance, 0.3 Da MS-MS tolerance, and the following variable modifications: carbamidomethylation and oxidation.

The search engine (Mascot) identifies potential hits within its database and calculates the probability of specific matches. We used a confidence interval, reported by AB Sciex software based on the Mascot results, of 95% or greater, which can be thought of as similar to Mascot  $p < 0.05$ , for identity.

**Immunoblotting**—Cells were rinsed with 1× PBS, and an appropriate amount of lysis buffer (1% Triton X-100, 2 mM EDTA, 4 mM Na<sub>3</sub>PO<sub>4</sub>, 100 mM NaCl, 10 mM MES, pH 5.8, 10 mM NaF, 1 protease inhibitor tablet) was added and lysed using a 21-gauge needle. Protein quantification was performed using the Bradford assay using protein assay dye reagent concentrate according to the manufacturer's instructions (Bio-Rad). Samples were prepared using 5× loading buffer (250 mM Tris-HCl, pH 6.8, 10% SDS, 30% glycerol, 0.02% bromophenol blue, 5%  $\beta$ -mercaptoethanol) and boiled for 5 min. The samples were electrophoresed in 7.5% polyacrylamide gels containing 0.1% SDS. Western transfer onto PVDF membrane was carried out using semi-dry transfer at 25 V for 1 h. 10% nonfat dry milk in TBS/Tween was used to block the membrane for 1 h and washed in TBS-T three times for 5 min each. The blots were incubated overnight at 4 °C with the appropriate amount of antibodies prepared in 1% milk. After three washes, the membrane was incubated with HRP-conjugated secondary antibody for 60 min at room temperature. Following secondary incubation, the blot was washed three times in TBS-T and incubated with the substrate (GE Healthcare) according to the manufacturer's instructions. The blots were exposed to Fuji Super RX-U Half-Speed Blue films (Brandywine Imaging Inc.) in the dark room. All Western blots were performed at least three times independently. Using the replicates, the data were analyzed using ImageLab™. This analysis is reported alongside all Western blot images.

**Immunostaining**—HEK293T cells were transiently transfected with the pBKCMV/NOD2Myc plasmid using Lipofectamine 2000 (Invitrogen). After overnight incubation, the cells were plated on 24-well dishes containing glass coverslips. Once the cells were attached to the coverslips, they were

washed two times with PBS. 4% paraformaldehyde solution in PBS was used for fixing the cells for 15 min at room temperature. The cells were then washed in PBS and treated with 0.3% Triton X-100 solution. Cells were treated with 5% normal goat serum for blocking and were incubated with rabbit monoclonal anti-Myc and mouse monoclonal anti-HSP70 antibodies. After overnight incubation, the cells were washed three times using PBS and incubated with Alexa Fluor-594 rabbit anti-goat and Alexa Fluor-488 mouse anti-goat sera. The cells were mounted on glass slides containing ProLong® gold antifade reagent with DAPI (Invitrogen).

**Half-life Determination**—Cycloheximide was used at a concentration of 100  $\mu$ g/ml, and the lysates were collected every 4 h. GGA, KNK437, or DMSO was incubated 2 h prior to the addition of cycloheximide. For plasmid-induced protein expression studies, cycloheximide was added, and lysates were collected after 2 days of transfection.

**Plasmid Construction**—HRSp-NOD2Myc was constructed by amplifying NOD2 from pBKCMV vector and ligated into HRSp vector. BglII and AsclI restriction sites were used to place the insert. The following primers were used to amplify NOD2: forward primer 5'-GAAGATCTGCCATGGGGGAAGAGG-GTGGT-3' and reverse primer 5'-TTGGCGCGCCTCACAG-ATCCTCTTCAGAGATGAG-3'. The ligated products were transformed using HB101 competent cells. pBKCMV-NOD2/702Myc, pBKCMV-NOD2/908Myc, and pBKCMV-NOD2/1007insCMyc were constructed by amplifying the inserts from pFASTBac vector containing the various NOD2 mutants (previously constructed using site-directed mutagenesis) and ligated into pBKCMV vector. The following primers were used to amplify NOD2: forward primer 5'-CGCGGATCCGCCAC-CATGGAGCAGAACTCATCTCTGAAGAGGATCTGAT-GGGGGAAGAGGGTTA-3' and reverse primer 5'-CCGCC-GCTCGAGTCAAAGCAAGAGTCTGGTGTCCCT-3'. BamHI and XhoI restriction sites were used to ligate the insert. The ligated products were transformed using DH5 $\alpha$  competent cells. The above primers were used to construct K2605/NOD2Myc lentiviral vector. The lentiviral vector was used to make stable cell line as described previously (34).

HSP70 was restriction-digested from pcDNA5/FRT/TO/HIS HSPA1A (Addgene, Plasmid 19537) using BamHI and XhoI restriction enzymes and ligated into pBKCMV vectors. The ligated products were transformed using DH5 $\alpha$  competent cells. The following primers were used to amplify the ATPase domain and the substrate binding domain of HSP70: 1) ATPase domain forward primer 5'-CGCGGATCCATGGATTACAAG-GATGACACGATAAGGCCAAAGCCGCGG-3'; 2) ATPase domain reverse primer 5'-GGCGGCCATCCTGATGGGGGAC-AAGTCCGAGTGAAGTTCGAGTTCGA-3'; 3) substrate binding domain forward primer 5'-CGCGGATCCATGGATTACAAG-GATGACGACGATAAGAACGTGCAGGACCTGCT-3'; and 4) substrate binding domain reverse primer 5'-TCGACTCGA-GCTAATCTACCTCCTCAATGGTGGGGCCTGACCCAG-ACC-3'. BamHI and XhoI enzymes were used to digest the inserts and pBKCMV vector. The ligated products were transformed using DH5 $\alpha$  competent cells. All the constructs were confirmed by DNA sequencing (GENEWIZ, Inc).

## HSP70 Regulates the Stability of NOD2

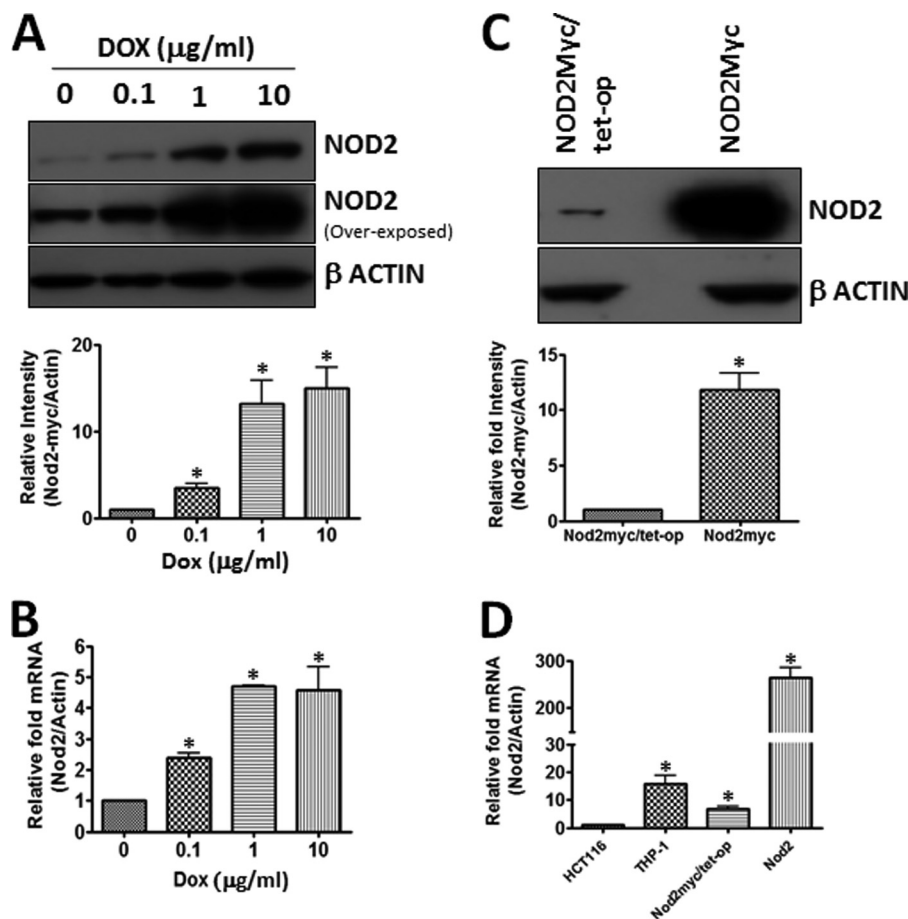


**FIGURE 1. Tetracycline-regulated NOD2-expressing cell lines.** *A*, cell lysates from HEK293T-NOD2Myc/Tet-op (tetracycline-regulated NOD2-expressing cell line) induced at different concentrations of doxycycline were probed for Myc antibody (1:1000) to detect the amount of NOD2 expressed. Actin (1:1000) was used as the loading control. Using the replicates, the bands were quantified using ImageLab™. *B*, RNA isolated from HEK293T-NOD2Myc/Tet-op (tetracycline-regulated NOD2-expressing cell line) induced at different concentrations of doxycycline were quantified for the amount of NOD2 mRNA using real time quantitative PCR. *C*, Western blot showing the difference in the level of NOD2 expression in HEK293T cells (NOD2Myc/Tet-op) no dox) and NOD2-overexpressed stable cell line (NOD2Myc). Myc and β-actin antibody (loading control) were used at a concentration of 1:1000. Western blots were performed on separate cell lysates at least three times. Using the replicates, the bands were quantified using ImageLab™. *D*, real time quantitative PCR used to measure the relative NOD2 levels in HCT 116, THP-1, HEK293T-NOD2Myc/Tet-op (no dox), and HEK293T-NOD2Myc cell lines. Results shown are the means ± S.D. of experiments performed in triplicate. \*,  $p < 0.05$  was considered as significant.

**Luciferase Reporter Assay**—Lipofectamine 2000 was used to transiently transfect HEK293T cells, and Lipofectamine LTX was used to transfect HCT 116. pGL4.32 (luc2P/NF-κB-RE/Hygro) and pRL *Renilla* luciferase reporter vectors were used. An appropriate amount of plasmids were mixed with the transfection reagent and incubated overnight in cells seeded in 24-well dishes. Cells were incubated with 2 µM MDP or 200 nM TNFα for 6 h, and the lysates were collected to perform the Dual-Luciferase Reporter Assay (Promega) according to the manufacturer's instructions and were normalized to *Renilla* activity. KNK437 or DMSO was treated 2 h prior to MDP stimulation.

**ELISA**—The media were collected and centrifuged at 200 × *g*, and the supernatant was subjected to ELISA (BD Biosciences) as per the manufacturer's instructions. MDP was stimulated for 6 h prior to media collection. KNK437 or DMSO was treated for 2 h prior to MDP stimulation. Appropriate plasmids were transfected using Lipofectamine 2000 a day before media collection.

**RT-PCR**—Total mRNA was isolated from the cells using a standard RNA extraction procedure (5'). mRNA was con-

verted to cDNA via the manufacturer's instructions using BioRad reverse transcriptase kit. Quantitative PCR was performed to detect the level of *NOD2* in various cDNAs. The following primers were used to identify *NOD2*: forward primer 5'-CGG-CGTTCCTCAGGAAGTAC-3' and reverse primer 5'-ACCC-CGGGCTCATGATG-3'. The following primers were used to identify actin in the PCR: forward primer 5'-GCTCGTCGTC-GACAACGGCTC-3' and reverse primer 5'-CAAACATGAT-CTGGGTCATCTTCTC-3'. Real time quantitative RT-PCRs were performed in ABI PRISM 7700 sequence detector (Applied Biosystems) according to the manufacturer's instruction. Samples were run in a 25-µl mixture in the following PCR condition: initial denaturation at 95 °C for 10 min, followed by 40 cycles, which consisted of 95 °C for 20 s, 60 °C for 30 s, 72 °C for 1 min, and a final extension at 72 °C for 10 min. The products were electrophoresed on a 1% agarose gel and visualized by staining the gel using ethidium bromide. The relative amount of *NOD2* mRNAs normalized to β-actin mRNA was calculated using the  $2^{-\Delta\Delta C_t}$  method (35).

**Data Analysis**—Data presented are means ± S.D. of at least three repeats. Each experiment (NF-κB promoter activity and

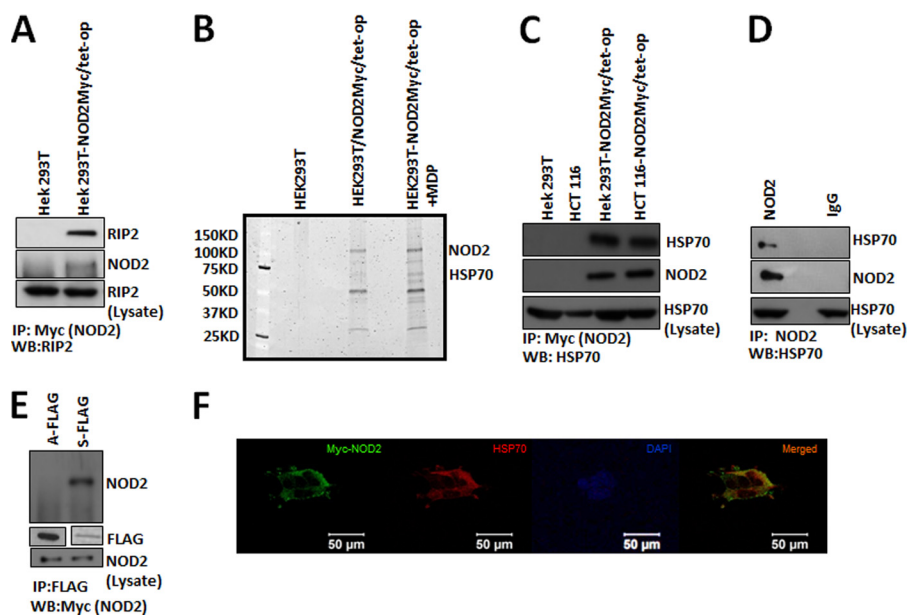


**FIGURE 2. Interaction between NOD2 and HSP70.** *A*, co-IP (*IP*) were performed using 1  $\mu$ l of mouse anti-Myc antibody per 150  $\mu$ l of lysate (HEK293T-NOD2Myc/Tet-op, stimulated with 2  $\mu$ M of MDP) and probed for RIP2 using rabbit anti-RIP2 antibody (1:1000). *WB*, Western blot. *B*, SYPRO<sup>®</sup>-stained 7.5% polyacrylamide gels showing the bands that were obtained through co-immunoprecipitation using mouse anti-Myc antibody in HEK293T, HEK293T-NOD2Myc/Tet-op (no dox), and HEK293T-NOD2Myc/Tet-op (no dox) cells stimulated with 2  $\mu$ M of MDP. The visible bands were characterized using protein mass spectrometry as described under the "Experimental Procedures." NOD2 and HSP70 were identified. *C*, co-IP performed using mouse anti-Myc antibody (1  $\mu$ l/150  $\mu$ l of lysate) in HEK293T-NOD2Myc/Tet-op (no dox), HCT 116-NOD2Myc/Tet-op (no dox), HEK293T, and HCT 116 cells and probed for HSP70 using rat anti-HSP70 antibody (1:1000) and rabbit anti-Myc antibody (1:1000). *D*, co-IP performed using rabbit NOD2 antiserum HM2559 (2  $\mu$ l/150  $\mu$ l) or rabbit IgG in THP-1 cells and probed for HSP70 using rat anti-HSP70 antibody (1:1000) and NOD2 using rabbit NOD2 antiserum HM2559 (1:5000). *E*, co-IP performed using mouse anti-FLAG antibody (5  $\mu$ l/150  $\mu$ l of lysate) in HEK293T cells transfected with pBKCMV/ATPase (*A-FLAG*) or pBKCMV/substrate binding domain (*S-FLAG*). Western blot was performed to detect NOD2 using Myc antibody (1:1000) and FLAG using FLAG antibody (1:500). *F*, HEK293T cells transiently transfected using pBKCMV/NOD2Myc vector and stained for NOD2 using mouse anti-Myc antibody (1:2000) and rabbit anti-HSP70. DAPI was used to stain the nucleus. *WB*, Western blot.

IL8 ELISA) was completed in at least four separate biological replicates ( $n = 4$ ). These biological replicates included studies of cells plated on separate dishes. Western blots were performed on separate cell lysates at least three times.

Student's *t* test was used to analyze difference between two groups. \*,  $p < 0.05$  was considered as significant.

## RESULTS

**Tetracycline-regulated NOD2 Expression**—Previous studies have successfully used immunoprecipitation followed by mass spectrometry to identify novel protein-protein interactions. In our hands, this approach yielded a significant number of proteins. We reasoned that this was due to the unnaturally high concentrations of NOD2 present in the cell, and perhaps many of these interactions were artifacts of our initial experimental design. Thus, we opted for a system where the expression of epitope-tagged NOD2 mirrored that of endogenous levels. Although antibodies for NOD2 already exist, we used epitope-tagged NOD2 on either its N or C terminus. We did this for two reasons as follows: 1) the tag could be used across many constructs of NOD2 (wild type, Crohn-associated variants, truncations, and protein domains of NOD2), and 2) steric occlusion of pre-existing NOD2 antibodies could prevent NOD2 from binding to its interacting proteins.

Using the protocol described by Blau and co-workers (28), we successfully constructed tunable NOD2 (containing Myc tag) stable cell line in HEK293T (Fig. 1*A*). We showed that NOD2 levels (both protein and mRNA) increased with an increasing

concentration of doxycycline (Fig. 1, *A* and *B*). It is not uncommon in the inducible cell lines to see leaking the promoter (*i.e.* expression of protein in the absence of doxycycline) (36). We observed low levels of NOD2 expression in the absence of doxycycline (Fig. 1, *A* and *B*). However, we thought that this very low expression of NOD2 might mirror the endogenously expressed cell line. We compared the expression of the regulated NOD2 (NOD2Myc/Tet-op (no doxycycline)) compared with the constitutively overexpressed NOD2 (NOD2Myc) in cell lines created by lentiviral vector K2605/NOD2 transduction. We found that NOD2 expression levels were over 257 times higher in the constitutively expressed system compared with the inducible system (Fig. 1, *C* and *D*). Moreover, we showed that the inducible expression system matched the expression of wild-type NOD2 in both THP-1, a monocyte cell line that endogenously expresses NOD2, and 2) HCT 116, an intestinal epithelium that has been shown to endogenously express NOD2 (Fig. 1*D*) (37). With the desired inducible NOD2 system in hand, we set out to identify novel protein interactors of NOD2.

**Identification of HSP70 as a NOD2 Interactor**—Using the NOD2 inducible cell lines, we performed immunoprecipitation followed by mass spectrometry. The experiment was performed in both the absence and presence of the NOD2 ligand MDP. No doxycycline was used in any of our experiments, as we showed that this amount of NOD2 best matches the endogenous levels (Fig. 1*D*). As a method to control for nonspecific interactions, several precautions were taken. First, we used

## HSP70 Regulates the Stability of NOD2

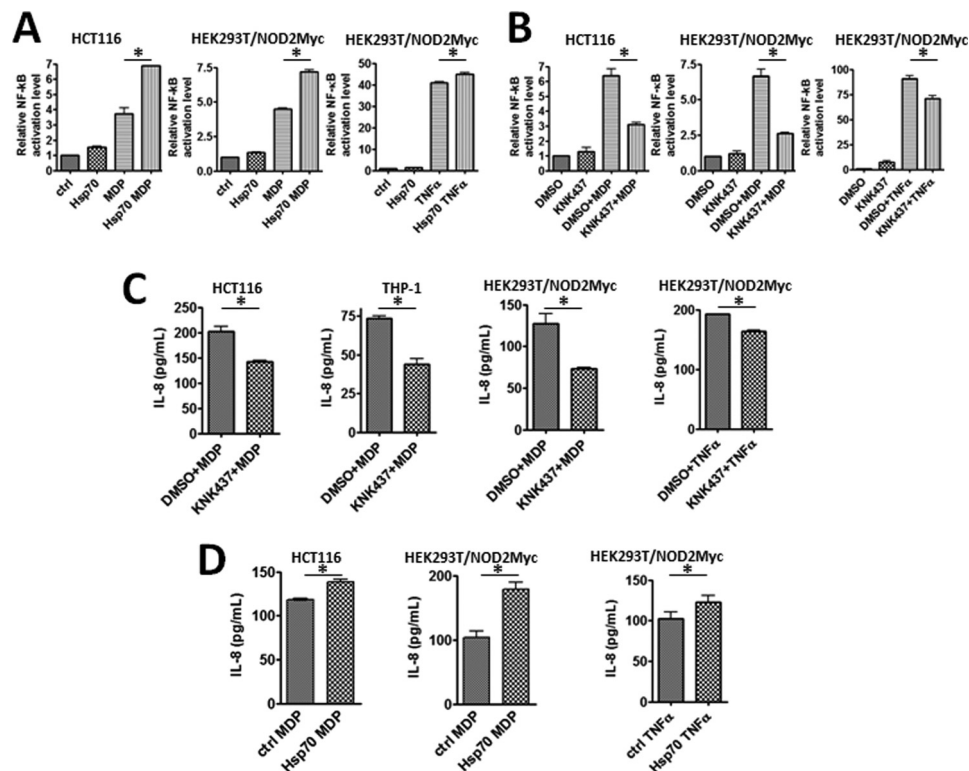


**FIGURE 3. HSP70 regulates NOD2 induced NF- $\kappa$ B signaling.** *A*, dual-luciferase assay performed on HEK293T/NOD2Myc and HCT 116 transfected with HSP70 or control vector in the presence or absence of 2  $\mu$ M MDP or 200 nM of TNF $\alpha$  incubated for 6 h. 75 ng of pGL432 and 7.5 ng of pRL vector was used per 24-well dish for transfection. Relative luciferase activity of firefly to *Renilla* is plotted. Results shown are the means  $\pm$  S.D. of experiments performed in quadruplicate. \*,  $p < 0.05$  was considered as significant. *B*, dual-luciferase assay performed on HEK293T/NOD2Myc and HCT 116 cells incubated with 100  $\mu$ M KNK437 or DMSO in the presence or absence of 2  $\mu$ M MDP or 200 nM TNF $\alpha$ . 75 ng of pGL432, 7.5 ng of pRL vector, and 200 ng of HSP70 or control vector were used per 24-well dish for transfection. Relative luciferase activity of firefly to *Renilla* is plotted. Results shown are the means  $\pm$  S.D. of experiments performed in triplicate. \*,  $p < 0.05$  was considered as significant. *C*, quantification using ELISA of the amount of IL-8 secreted by HCT 116, THP-1, and HEK293T/NOD2Myc cells incubated with 2  $\mu$ M MDP or 200 nM TNF $\alpha$  in the presence of 100  $\mu$ M KNK437 or DMSO. Results shown are the means  $\pm$  S.D. of experiments performed in triplicate. \*,  $p < 0.05$  was considered as significant. *D*, quantification using ELISA of the amount of IL-8 secreted by HEK293T/NOD2Myc and HCT 116 cells transfected with HSP70 or control vector incubated with 2  $\mu$ M MDP or 200 nM TNF $\alpha$ . Results shown are the means  $\pm$  S.D. of experiments performed in triplicate. \*,  $p < 0.05$  was considered as significant.

HEK293T cells that did not express an epitope-tagged NOD2. Second, we performed extensive washing (four washes with increasing concentration of sodium chloride, see “Experimental Procedures” for more details) of the resin to ensure nonspecific proteins were removed. Finally, we selectively eluted NOD2 from the resin using low concentrations of Myc peptide. To validate our method, we first confirmed the presence of a known NOD2 interactor, RIP2 (Fig. 2A). Upon confirming our method, the interacting proteins were separated using SDS-PAGE, and proteins were detected using Sypro Ruby<sup>®</sup> stain (Fig. 2B). Prominent bands were excised from the gel, trypsinized, and analyzed using electrospray ionization-mass spectrometry. In total, we identified six protein-protein interactors using mass spectrometry. Two of these proteins have already been identified as NOD2 interactors, actin and HSP90.

Initially, we thought that the interaction of NOD2 and HSP70 might be an artifact of our experiment, as HSP70 is ubiquitously expressed in cells (38). However, HSP70 has recently been shown to control the innate immune system both by binding and inhibiting TLR4, as well as mediating decreases in lipoteic acid and TNF $\alpha$ -induced signaling (39–41). Thus, we were intrigued by the role that HSP70 could potentially play in regulating NOD2. We set out to validate our initial results.

First, we performed an IP experiment in the HEK293T-NOD2Myc/tet-op (no dox stimulation) cell line and HCT 116-NOD2Myc/tet-op (no dox stimulation). We confirmed that NOD2 interacted with HSP70 using Myc antibodies to immunopurify both cell lines (Fig. 2C). Next we assayed whether THP-1 cells, which endogenously express NOD2, interacted in HSP70. We found that HSP70 was immunopurified in these cells (Fig. 2D). To determine what portion of HSP70 interacts with NOD2, we expressed the two prominent domains of HSP70 as epitope tags, the ATP binding domain and substrate binding domain. Using co-immunoprecipitation, we detected an interaction with only NOD2 in the substrate binding domain, leading us to believe that NOD2 interacts with HSP70 (Fig. 2E). In addition, immunostaining followed by confocal microscopy confirms that HSP70 and NOD2 interact in the cell (Fig. 2F). Thus, these data support that NOD2 interacts with HSP70 under physiological conditions. We were now curious to determine the function of this interaction in the context of innate immune signaling.

**HSP70 Regulates NOD2-induced NF- $\kappa$ B Activity**—NOD2 is known to activate the NF- $\kappa$ B pathway upon stimulation from bacterial cell wall ligands (12, 15). A ligand for NOD2 is MDP.

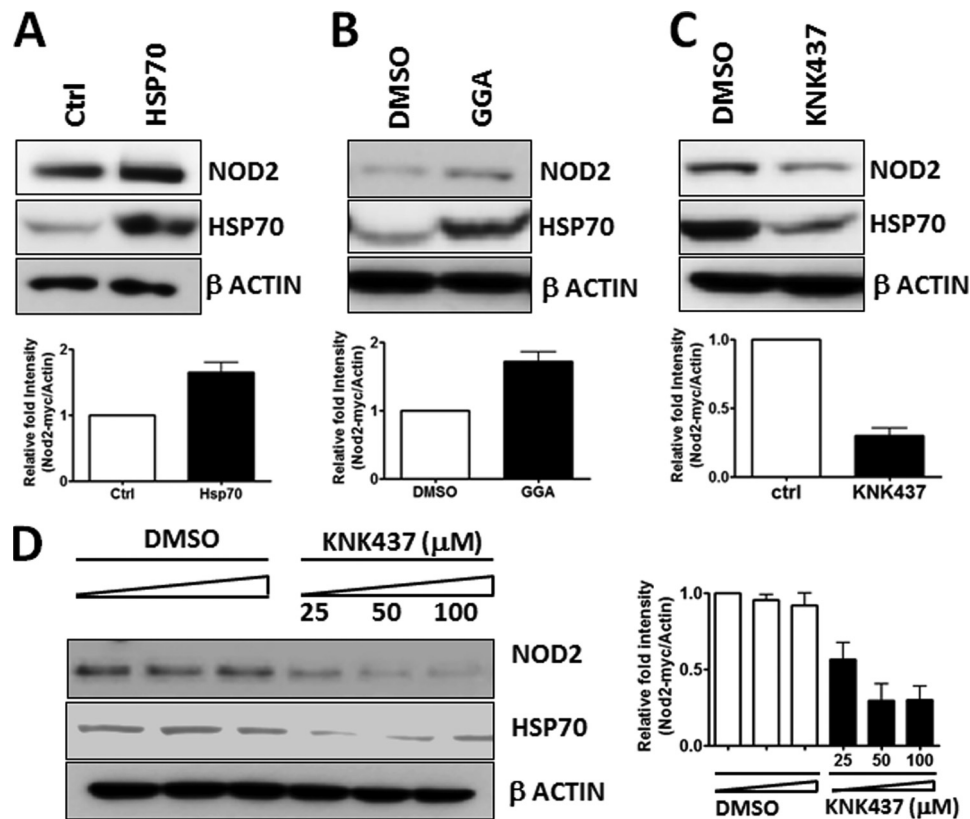


**FIGURE 4. HSP70 regulates NOD2 level in the cell.** *A*, cell extracts from HSP70 or control vector-transfected HEK293T/NOD2Myc cells were probed using rabbit anti-Myc antibody (1:1000) and rabbit anti-HSP70 antibody (1:1000).  $\beta$ -Actin (1:1000) was used as a loading control. *B*, cell extracts of HEK293T-NOD2-Myc/Tet-op cells incubated with 100  $\mu$ M of GGA or DMSO were probed using rabbit anti-Myc antibody (1:1000) and rabbit anti-HSP70 antibody (1:1000).  $\beta$ -Actin (1:1000) was used as a loading control. *C*, cell extracts of HEK293T-NOD2-Myc/Tet-op cells incubated with 100  $\mu$ M KNK437 or DMSO was probed using rabbit anti-Myc antibody (1:1000) and rabbit anti-HSP70 antibody (1:1000).  $\beta$ -Actin (1:1000) was used as a loading control. *D*, cell extracts of HEK293T-NOD2-Myc/Tet-op cells incubated with 25, 50, or 100  $\mu$ M of KNK437 or DMSO were probed using rabbit anti-Myc antibody (1:1000).  $\beta$ -Actin (1:1000) was used as a loading control. Western blots were performed on separate cell lysates at least three times. Using the replicates, the bands were quantified using ImageLab™.

We hypothesized that HSP70 plays a role in NOD2's ability to signal through the NF- $\kappa$ B pathway. To test this hypothesis, we took a multipronged approach, overexpressing *and* decreasing the levels of HSP70 within the cell. We then analyzed the ability of NOD2 to induce NF- $\kappa$ B activation using the established luciferase NF- $\kappa$ B reporter assay. Briefly, this assay is a transfection assay in which the NF- $\kappa$ B promoter drives the expression of luciferase. When NF- $\kappa$ B is activated, higher levels of luciferase are expected. Previously, it has been shown that overexpression of HSP70 decreases the ability of TLR4 to signal via NF- $\kappa$ B. Our results showed that NOD2 increased NF- $\kappa$ B activation when HSP70 was overexpressed in both NOD2-transfected (HEK293T) and a cell line containing endogenous NOD2 (HCT 116) (Fig. 3A). We saw no difference in NF- $\kappa$ B activation when HSP70 was overexpressed but not treated with MDP; thus, overexpression of HSP70 does not activate NF- $\kappa$ B (Fig. 3A). The difference in NF- $\kappa$ B activation was only present after the cells were stimulated with MDP. We also showed that the effect could be reversed by decreasing the expression of HSP70 (Fig. 3B). KNK437 is a small molecule that has been shown to specifically inhibit HSP70 at the mRNA level (42). When HCT 116 cells were treated with KNK437, we observed a decrease in the level of HSP70 mRNA (data not shown), and the same trend was observed in HEK293T-NOD2Myc/tet-op (no dox stimulation) (Fig. 4, C and D). Using the same luciferase assay described

above, we observed that NOD2's ability to signal the NF- $\kappa$ B pathway via MDP was significantly decreased when treated with HSP70 inhibitor (Fig. 3B). When the cells were treated with the inhibitor alone, there was no significant change in NF- $\kappa$ B activation. As a control, cells were also treated with TNF $\alpha$ , a known NF- $\kappa$ B activator (43). HSP70 overexpression and treatment with TNF $\alpha$  yielded a 9.7% increase in NF- $\kappa$ B activation, and treatment with KNK437 showed a 22.4% decrease in NF- $\kappa$ B activation. As a comparison, MDP showed a 59.9% increase upon HSP70 overexpression and 60.5% decrease upon KNK437 treatment. These data demonstrate that HSP70 regulates NOD2's ability to signal to NF- $\kappa$ B.

To further support our data, we assayed NOD2's ability to produce cytokines in both HSP70 overexpression or inhibition conditions. This assay avoided the use of the transfection of the reporter plasmid. Our data showed that IL-8, a pro-inflammatory cytokine that is known to be produced upon NOD2 activation, decreased in the presence of the HSP70 inhibitor in three cell lines (HCT 116, THP-1, and HEK293T-NOD2 NOD2Myc/Tet-op (Fig. 3C)). In addition, when HSP70 was overexpressed, the levels of IL-8 increased when stimulated with MDP (Fig. 3D). Again, TNF $\alpha$  was used as a control, and we saw the same trends as with the Dual-Luciferase assay. HSP70 overexpression and treatment with TNF $\alpha$  yielded a 19.7% increase in the amount of IL-8 secreted, and treatment with

## HSP70 Regulates the Stability of NOD2

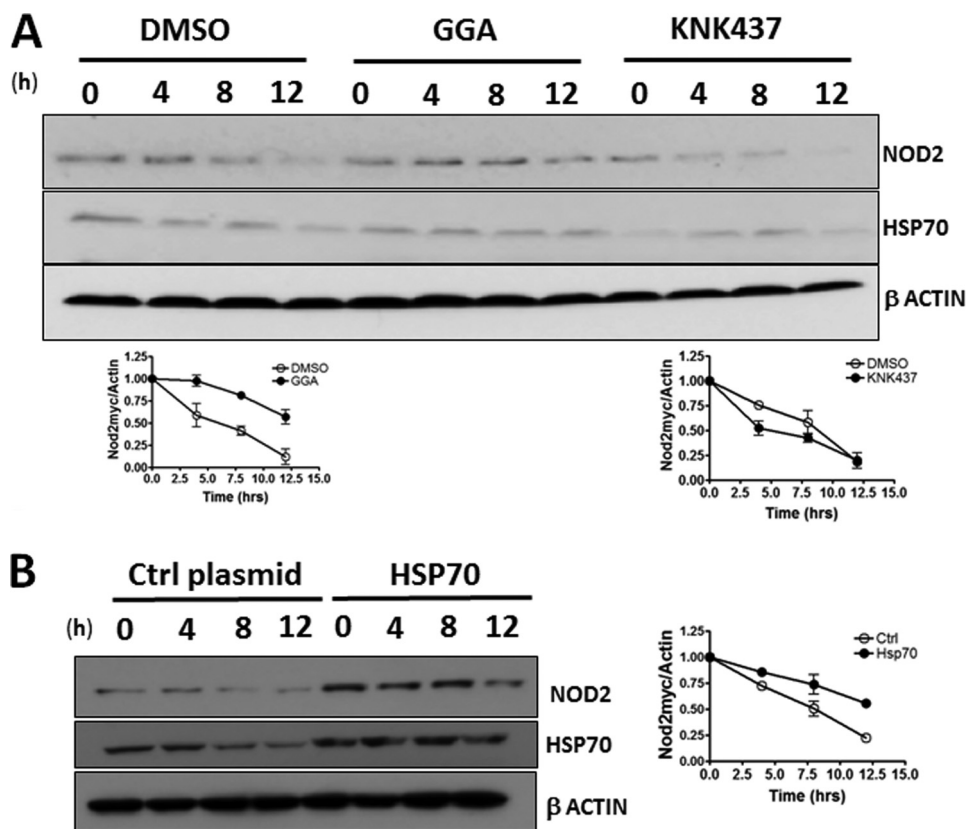


**FIGURE 5. HSP70 regulates NOD2's stability in the cell.** *A*, HEK293T-NOD2Myc/Tet-op cells were incubated with 100  $\mu$ M GGA or 100  $\mu$ M KNK437 or DMSO for 2 h, and lysates were collected after cycloheximide treatment during the indicated time intervals. Equal amounts of lysates were subjected to Western blot and probed using rabbit anti-Myc antibody (1:1000) or rabbit anti-HSP70 antibody (1:1000).  $\beta$ -Actin (1:1000) was used as a loading control. Relative amount of NOD2Myc to  $\beta$ -actin was plotted as the means  $\pm$  S.D. from three independent experiments. *B*, cell extracts from HEK293T-NOD2Myc/Tet-op cells, transfected with HSP70 or control vector, and treated with cycloheximide. Cell lysates were collected during the indicated time intervals and subjected to Western blot and probed using rabbit anti-Myc antibody (1:1000) or rabbit anti-HSP70 antibody (1:1000).  $\beta$ -Actin (1:1000) was used as a loading control. Relative amount of NOD2Myc to  $\beta$ -actin was plotted as the means  $\pm$  S.D. from three independent experiments. Western blots were performed on separate cell lysates at least three times. Using the replicates, the bands were quantified using ImageLab<sup>TM</sup>.

KNK437 showed a 14.8% decrease in the amount of IL-8 secreted. As a comparison, MDP showed a 71.9% increase upon HSP70 overexpression and 42.3% decrease upon KNK437 treatment. These data confirm our hypothesis that HSP-70 positively regulates NOD2's ability to signal in the presence of bacterial cell wall ligands. We next aimed to determine the mechanism by which HSP70 regulates NOD2.

**HSP70 Regulates NOD2 Level in Cells**—HSP70 is a chaperone and has the ability to stabilize proteins (44, 45). We wondered whether HSP70 was affecting NOD2's stability in the cell. To test whether HSP70 alters NOD2 levels in the cell, we used three different conditions to control the expression of HSP70 as follows: 1) overexpression of HSP70 using transfection; 2) overexpression of HSP70 using the small molecule inducer GGA; and 3) inhibition of HSP70 with KNK437 (Fig. 4, A–C). We analyzed NOD2's protein level using immunoblotting. Overexpression of HSP70 showed an increase in NOD2 levels (Fig. 4, A and B), and decreasing HSP70 showed a decrease in NOD2 levels (Fig. 4C). Moreover, we showed that the decrease in HSP70 using the small molecule inhibitor was dose-dependent (Fig. 4D). As the inhibitor concentration was increased, the concentration of HSP70 decreased as expected, and the amount of NOD2 also decreased. These data could explain the NOD2 signaling effects in changing concentrations of HSP70 (Fig. 3).

Thus, one can control NOD2 signaling by changing the concentration of HSP70 in the cell.

**HSP70 Regulates NOD2 Half-life**—As HSP70 is able to affect the level of NOD2 in the cell, it should change the half-life of NOD2 in the cell. We performed the classical protein half-life experiment using cycloheximide, a well documented translational inhibitor (46). Again, we used three approaches to control the levels of HSP70 as follows: small molecule activator, small molecule inhibitor, and overexpression using transfection. We showed that when HSP70 was overexpressed using GGA, there was a 2-fold increase in NOD2's half-life (Fig. 5A). Conversely, when HSP70 was inhibited using KNK437, there was a 2-fold decrease in Nod's half-life (Fig. 5A). When the level of HSP70 was increased using transfection, again the level of NOD2 increased 2-fold (Fig. 5B). These data support that HSP70 is able to stabilize NOD2 and thereby directly affect its ability to signal.

**Decreased Stability of NOD2 Crohn Mutants**—It has previously been shown that the NOD2 Crohn-associated variants are defective in their ability to signal the presence of bacterial cell wall fragments via NF- $\kappa$ B (12, 22). We hypothesized that this difference is due to the inherent stability of the mutants as compared with the wild type. We used two approaches to quantify the stability of the NOD2 Crohn mutants. First, we transfected



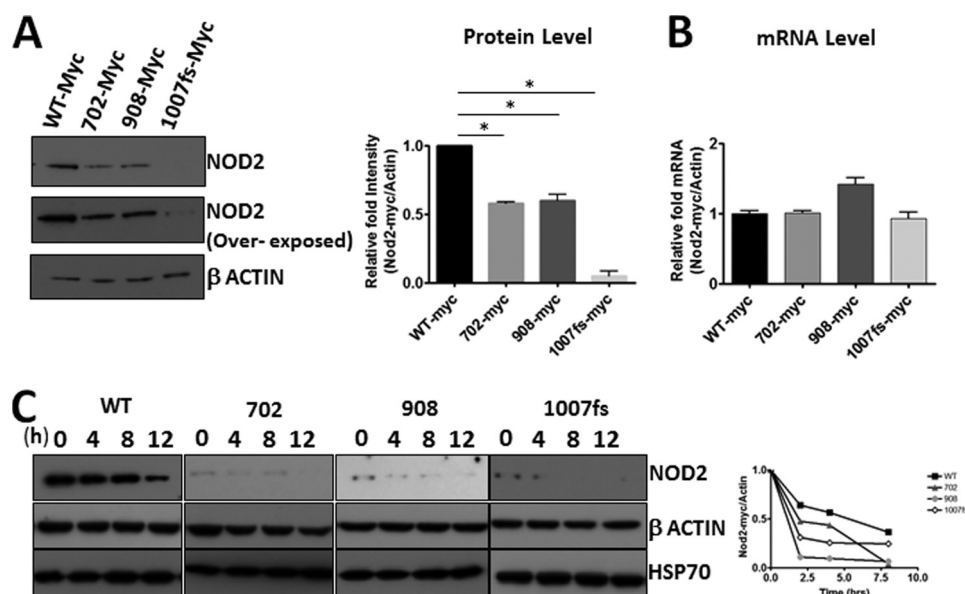


**FIGURE 6. Reduced expression of the NOD2 Crohn mutants.** *A*, cell lysates from HEK293T cells transfected with 1  $\mu$ g of pBKCMV/NOD2Myc, pBKCMV-NOD2/702Myc, pBKCMV-NOD2/908Myc, or pBKCMV-NOD2/1007insCMyc vectors were probed for Myc using rabbit anti-Myc antibody (1:1000).  $\beta$ -Actin (1:1000) was used as a loading control. *B*, RNA isolated from HEK293T cells transfected with 1  $\mu$ g of pBKCMV/NOD2Myc, pBKCMV-NOD2/702Myc, pBKCMV-NOD2/908Myc, or pBKCMV-NOD2/1007insCMyc vectors were reverse-transcribed to cDNA and used to perform quantitative real time PCR using NOD2 and actin primers. The relative amount of NOD2 to actin levels were plotted as the means  $\pm$  S.D. from three independent experiments. *C*, HEK293T cells transfected with 1  $\mu$ g of pBKCMV/NOD2Myc, pBKCMV-NOD2/702Myc, pBKCMV-NOD2/908Myc, or pBKCMV-NOD2/1007insCMyc vectors and treated with cycloheximide. The lysates were collected at the indicated time intervals. Equal amounts of lysates were subjected to Western blot and probed using rabbit anti-Myc antibody (1:1000) or rabbit anti-HSP70 (1:1000).  $\beta$ -Actin (1:1000) was used as a loading control. Relative amount of NOD2Myc to  $\beta$  actin was plotted as the means  $\pm$  S.D. from three independent experiments. \*,  $p < 0.05$  was considered as significant. Western blots were performed on separate cell lysates at least three times. Using the replicates, the bands were quantified using ImageLab™.

cells with equal amounts of either wild-type NOD2 or Crohn-associated NOD2 variants. The cells were harvested and subsequently analyzed for NOD2 using Western blot and mRNA using RT-PCR (Fig. 6, *A* and *B*). We found that the mutants were expressed significantly less than the wild type, even though they have the same amount of mRNA expressed in the cell. Interestingly, the frameshift NOD2 Crohn variant showed a severe decrease in protein levels. This variant is linked to a more detrimental phenotype in humans affected with Crohn disease. To support the idea that the Crohn mutants were unstable compared with the wild type, we performed the half-life experiments with the mutants. We found that the half-life of the mutants was significantly decreased compared with the wild type (Fig. 6C). This instability could provide an explanation of why the Crohn mutants cannot properly signal as efficiently as the wild type. We hypothesized that the Crohn mutants interact with HSP70, the protein that can affect the stability of wild-type NOD2.

**Increasing HSP70, Rescues NOD2 Mutant Activity**—To determine whether the Crohn mutants were capable of interacting with HSP70, we performed co-immunoprecipitation with HSP70 (Fig. 7A). Although we have previously shown that the mutant expression was less than the wild type (Fig. 6A), we expected that the immunoprecipitation would be enriched for low levels of protein. We showed that all three mutants were able to purify endogenous HSP70. In addition, we probed whether overexpression of HSP70 would affect the level of the NOD2 mutants. When HSP70 is overexpressed using transfection, the levels of the Crohn mutants also increased in cells (Fig. 7B). Given that HSP70 increased both the stability and the abil-

ity for wild-type NOD2 to signal via NF- $\kappa$ B, we assayed whether HSP70 had the same effect on the Crohn mutants of NOD2. When HSP70 was overexpressed using transfection, we showed that the ability Crohn mutants' to signal the presence of the bacterial cell wall ligand, MDP, was significantly increased (Fig. 7C). In two of the three Crohn-associated NOD2 variants, the level of NF- $\kappa$ B activation was restored to wild-type levels. These data imply that HSP70 is able to rescue the ability of the Crohn mutants to signal.

## DISCUSSION

NOD2 is an important innate immune receptor that is responsible for sensing the occurrence of bacterial cell wall fragments within mammalian cells. It has been known for over 10 years that mutations in NOD2 correlate to the development of Crohn disease (11). Moreover, these mutations do not properly respond to bacterial cell wall components (12). Studies have shown that when cells containing the NOD2 mutations are treated with the bacterial cell wall fragments, a lower NF- $\kappa$ B response is obtained (12, 22). It has been suggested that a basal level of NOD2 activation is needed in the cell to control other innate immune receptors. Without the ability to activate NF- $\kappa$ B, an uncontrollable amount of inflammation ensues, and Crohn disease develops (47, 48). Much effort has been focused on trying to identify the mechanism by which NOD2 signals to the NF- $\kappa$ B response. Many protein interactors have been found. However, none explain the Crohn NOD2 phenotype, *i.e.* a lack of response to bacterial cell wall ligand.

To understand the mechanism of NOD2 signaling, we developed a novel system to screen for NOD2 protein-protein inter-

## HSP70 Regulates the Stability of NOD2

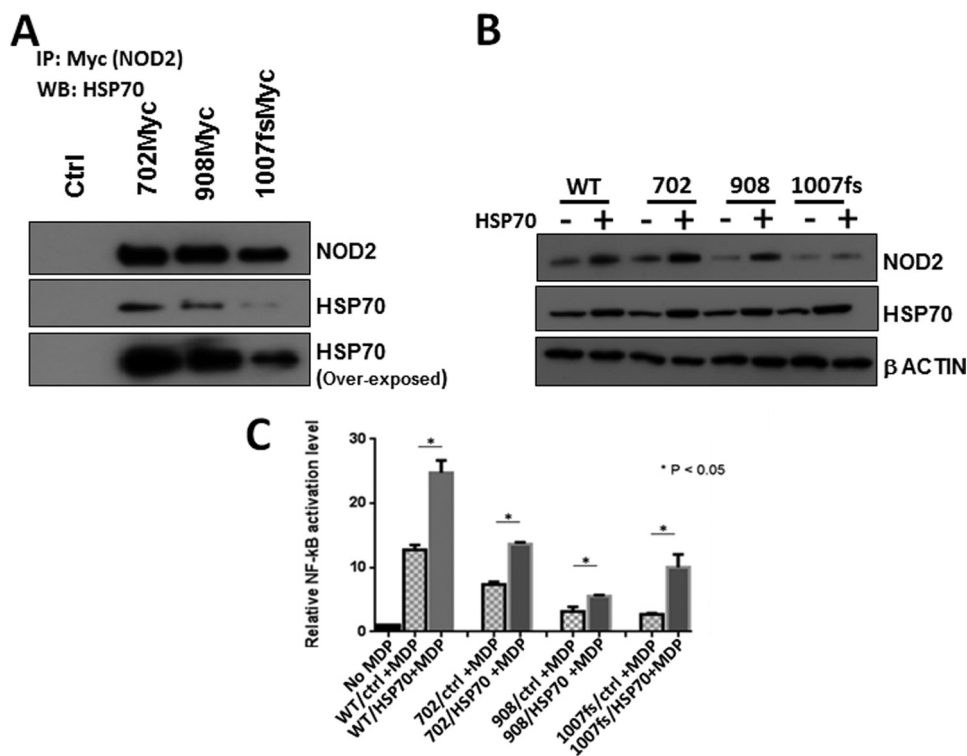


**FIGURE 7. HSP70 regulates NOD2 Crohn mutant activity.** *A*, co-immunoprecipitation was performed in HEK293T cells transfected with 1  $\mu$ g of pBKMV, pBKMV-NOD2/702Myc, pBKMV-NOD2/908Myc, and pBKMV-NOD2/1007insCMyc vectors, using 1  $\mu$ g of mouse anti-Myc antibody per 150  $\mu$ l of cell lysate. Eluates were probed for HSP70 using 1:1000 of rat anti-HSP70 and rabbit anti-Myc antibody. *B*, cell lysates from HEK293T cells transfected with 750 ng of pBKMV/NOD2Myc, pBKMV-NOD2/702Myc, pBKMV-NOD2/908Myc, or pBKMV-NOD2/1007insCMyc vectors along with 1  $\mu$ g of HSP70 or control vector were probed using 1:1000 rabbit anti-Myc antibody and 1:1000 rabbit anti-HSP70 antibody.  $\beta$ -Actin was used as a loading control. Western blots were performed on separate cell lysates at least three times. Using the replicates, the bands were quantified using ImageLab<sup>TM</sup>. *C*, dual-luciferase assays were performed on HEK293T cells transfected with 50 ng of pBKMV/NOD2Myc, pBKMV-NOD2/702Myc, pBKMV-NOD2/908Myc, or pBKMV-NOD2/1007insCMyc vectors along with 50 ng of HSP70 or control vector/NOD2Myc and HCT 116 transfected with HSP70 or control vector in the presence or absence of 2  $\mu$ M MDP. 10 ng of pGL432 and 1 ng of pRL vector were used per 24-well dish for transfection. Relative luciferase activity of firefly to *Renilla* is plotted. Results shown are the means  $\pm$  S.D. of experiments performed in triplicates. \*,  $p < 0.05$  was considered as significant.

actors. Our approach has two main advantages over previous NOD2 studies. First, a tetracycline-inducible promoter system allowed a controllable, low level expression of NOD2 to be obtained (Fig. 1A). Second, the expression of an epitope-tagged NOD2 allowed for the efficient purification of NOD2 and the interacting proteins (Fig. 2B). The interacting proteins could then be identified using mass spectrometry. Our small screen identified HSP70 as a protein that interacts with NOD2. Initially, we were skeptical of the significance of this finding, as HSP70 is ubiquitously expressed in the cells, and we believed that this finding could be an artifact. However, recently HSP70 has been shown to regulate a number of innate immune receptors. Our study went on to validate HSP70 as a genuine NOD2 protein-protein interactor (Fig. 1, A and C). We showed that NOD2 interacts with the substrate binding domain of HSP70 (Fig. 2E). We investigated the role of HSP70 in NOD2 signaling using established cell-based assays to monitor NF- $\kappa$ B activation (Fig. 3, A and B). We observed that overexpression of HSP70 yielded an increase in NOD2's ability to signal when stimulated with MDP. The literature has reported that overexpression of HSP70 blocks the denaturation of I $\kappa$ B kinase thereby increasing the nuclear translocation of NF- $\kappa$ B (49). This could explain the increase in TNF $\alpha$ -induced NF- $\kappa$ B signaling upon HSP70 overexpression. However, the degree of NOD2 activation via MDP upon HSP70 overexpression was higher, compared with the

TNF $\alpha$ -induced activation (Fig. 3A), implying that more than just I $\kappa$ B kinase stabilization was necessary for the increase. We went on to show that HSP70 increases the half-life of NOD2 (Fig. 5, A and B). At this point, we wondered whether the half-life of the Crohn mutants was relative to the wild-type NOD2. We found that the Crohn mutants are inherently unstable, and their half-life is less than that of the wild-type protein (Fig. 6, A–C). This fact intrigued us, and we investigated whether the overexpression of HSP70 could provide a rescue mechanism for the NOD2 Crohn mutants, as the Crohn mutants also interact with HSP70 (Fig. 7A). We found that overexpression of HSP70 was able to restore the ability of the Crohn mutants to signal upon stimulation with MDP (Fig. 7C).

Overexpression of HSP70 to rescue a protein's function is not a new phenomenon. There are many examples in the literature supporting this idea. For example, p53 and mutants of this protein are protected from degradation in the presence of excess HSP70 (50). In addition, human ether-a-go-go-related gene, a subunit of the potassium current I protein, is stabilized when HSP70 is overexpressed (51). Moreover, this study shows another protein (human ether-a-go-go-related gene) that HSP70 is capable of rescuing in its mutated form. An exciting outcome of our findings is that it suggests a potential method to treat Crohn disease, a small molecule that can specifically stabilize NOD2, by acting as a surrogate for the HSP70 protein.

Our study complements the finding by Kobayashi and co-workers (24) that NOD2 is rapidly degraded in the presence of MDP, as HSP90 is released. We found that NOD2 interacts with HSP70 independent of the presence of MDP, its bacterial cell wall ligand. Thus, HSP70 may provide a mechanism to reinitiate the ability of NOD2 to signal when there is a new burst of bacterial cell wall ligands. If, however, NOD2 is mutated, it is unable to signal the presence of bacterial cell wall fragments as its half-life in the cell is decreased. We found that overexpression of HSP70 is able to rescue NOD2's response to bacterial cell wall ligands. We propose that HSP90 could play a similar role, and we are currently working to determine whether HSP90 interacts with the Crohn mutants. This mechanism is different from HSP70's ability to alter the ability of TLR to signal. HSP70 (39) has been shown to specifically down-regulate the TLR4 response to lipopolysaccharide (39). Thus, the cell has designed HSP70 to be both an activator and an inhibitor of innate immune signaling.

In conclusion, we have developed a tetracycline-inducible NOD2 expression system that has allowed us to control the expression of NOD2 and purify interacting proteins. We have identified HSP70 as a novel NOD2 protein interactor. HSP70 is able to increase the half-life of NOD2 in the cell, and it also restores the response of the Crohn-associated NOD2 mutants. We propose that small molecules that can specifically stabilize the NOD2 Crohn mutants may be useful in the treatment of Crohn disease.

*Acknowledgments*—We acknowledge Dr. John C. Kappes (University of Alabama, Birmingham) for kindly providing lentiviral vector K2605. We acknowledge Leila Choe and Professor Kelvin Lee at the University of Delaware Proteomics and Mass Spectrometry Facility, which is supported in part by the Delaware IDeA Network of Biomedical Research Excellence, National Institutes of Health Grant 8 P20 GM103446-13, for the mass spectrometry and protein identification. We thank Dr. Brian Bahnson and Amy Schaefer for critical reading of the manuscript.

## REFERENCES

- Janeway, C. A., Jr., and Medzhitov, R. (2002) Innate immune recognition. *Annu. Rev. Immunol.* **20**, 197–216
- Akira, S., Uematsu, S., and Takeuchi, O. (2006) Pathogen recognition and innate immunity. *Cell* **124**, 783–801
- Medzhitov, R. (2007) Recognition of microorganisms and activation of the immune response. *Nature* **449**, 819–826
- Tosi, M. F. (2005) Innate immune responses to infection. *J. Allergy Clin. Immunol.* **116**, 241–249
- Wright, S. D. (1999) Toll, a new piece in the puzzle of innate immunity. *J. Exp. Med.* **189**, 605–609
- Imler, J. L., and Hoffmann, J. A. (2001) Toll receptors in innate immunity. *Trends Cell Biol.* **11**, 304–311
- Brodsky, I., and Medzhitov, R. (2007) Two modes of ligand recognition by TLRs. *Cell* **130**, 979–981
- Martinon, F., and Tschopp, J. (2005) NLRs join TLRs as innate sensors of pathogens. *Trends Immunol.* **26**, 447–454
- Kinnebrew, M. A., and Pamer, E. G. (2012) Innate immune signaling in defense against intestinal microbes. *Immunol. Rev.* **245**, 113–131
- Abraham, C., and Medzhitov, R. (2011) Interactions between the host innate immune system and microbes in inflammatory bowel disease. *Gastroenterology* **140**, 1729–1737
- Ogura, Y., Bonen, D. K., Inohara, N., Nicolae, D. L., Chen, F. F., Ramos, R., Britton, H., Moran, T., Karaliuskas, R., Duerr, R. H., Achkar, J. P., Brant, S. R., Bayless, T. M., Kirschner, B. S., Hanauer, S. B., Nuñez, G., and Cho, J. H. (2001) A frameshift mutation in NOD2 associated with susceptibility to Crohn's disease. *Nature* **411**, 603–606
- Inohara, N., Ogura, Y., Fontalba, A., Gutierrez, O., Pons, F., Crespo, J., Fukase, K., Inamura, S., Kusumoto, S., Hashimoto, M., Foster, S. J., Moran, A. P., Fernandez-Luna, J. L., and Nuñez, G. (2003) Host recognition of bacterial muramyl dipeptide mediated through NOD2. Implications for Crohn's disease. *J. Biol. Chem.* **278**, 5509–5512
- Borzutzky, A., Fried, A., Chou, J., Bonilla, F. A., Kim, S., and Dedeoglu, F. (2010) NOD2-associated diseases: Bridging innate immunity and autoinflammation. *Clin. Immunol.* **134**, 251–261
- Lesage, S., Zouali, H., Cézard, J. P., Colombel, J. F., Belaiche, J., Almer, S., Tysk, C., O'Morain, C., Gassull, M., Binder, V., Finkel, Y., Modigliani, R., Gower-Rousseau, C., Macry, J., Merlin, F., Chamailard, M., Jannot, A. S., Thomas, G., Hugot, J. P., EPWG-IBD Group, EPIMAD Group, and GETAID Group (2002) CARD15/NOD2 mutational analysis and genotype-phenotype correlation in 612 patients with inflammatory bowel disease. *Am. J. Hum. Genet.* **70**, 845–857
- Ogura, Y., Inohara, N., Benito, A., Chen, F. F., Yamaoka, S., and Nunez, G. (2001) NOD2, a Nod1/Apaf-1 family member that is restricted to monocytes and activates NF- $\kappa$ B. *J. Biol. Chem.* **276**, 4812–4818
- Gutierrez, O., Pipaon, C., Inohara, N., Fontalba, A., Ogura, Y., Prosper, F., Nunez, G., and Fernandez-Luna, J. L. (2002) Induction of NOD2 in myelomonocytic and intestinal epithelial cells via nuclear factor- $\kappa$ B activation. *J. Biol. Chem.* **277**, 41701–41705
- Ogura, Y., Lala, S., Xin, W., Smith, E., Dowds, T. A., Chen, F. F., Zimmermann, E., Tretiakova, M., Cho, J. H., Hart, J., Greenson, J. K., Keshav, S., and Nuñez, G. (2003) Expression of NOD2 in Paneth cells: a possible link to Crohn's ileitis. *Gut* **52**, 1591–1597
- Grimes, C. L., Ariyananda Lde, Z., Melnyk, J. E., and O'Shea, E. K. (2012) The innate immune protein NOD2 binds directly to MDP, a bacterial cell wall fragment. *J. Am. Chem. Soc.* **134**, 13535–13537
- Mo, J., Boyle, J. P., Howard, C. B., Monie, T. P., Davis, B. K., and Duncan, J. A. (2012) Pathogen sensing by nucleotide-binding oligomerization domain-containing protein 2 (NOD2) is mediated by direct binding to muramyl dipeptide and ATP. *J. Biol. Chem.* **287**, 23057–23067
- Abbott, D. W., Wilkins, A., Asara, J. M., and Cantley, L. C. (2004) The Crohn's disease protein, NOD2, requires RIP2 in order to induce ubiquitylation of a novel site on NEMO. *Curr. Biol.* **14**, 2217–2227
- Strober, W., Murray, P. J., Kitani, A., and Watanabe, T. (2006) Signaling pathways and molecular interactions of NOD1 and NOD2. *Nat. Rev. Immunol.* **6**, 9–20
- Bonen, D. K., Ogura, Y., Nicolae, D. L., Inohara, N., Saab, L., Tanabe, T., Chen, F. F., Foster, S. J., Duerr, R. H., Brant, S. R., Cho, J. H., and Nuñez, G. (2003) Crohn's disease-associated NOD2 variants share a signaling defect in response to lipopolysaccharide and peptidoglycan. *Gastroenterology* **124**, 140–146
- McDonald, C., Chen, F. F., Ollendorff, V., Ogura, Y., Marchetto, S., Lécine, P., Borg, J. P., and Nuñez, G. (2005) A role for Erbin in the regulation of NOD2-dependent NF- $\kappa$ B signaling. *J. Biol. Chem.* **280**, 40301–40309
- Lee, K. H., Biswas, A., Liu, Y. J., and Kobayashi, K. S. (2012) Proteasomal degradation of NOD2 protein mediates tolerance to bacterial cell wall components. *J. Biol. Chem.* **287**, 39800–39811
- Richmond, A. L., Kabi, A., Homer, C. R., Marina-García, N., Nickerson, K. P., Nesvizhskii, A. I., Sreekumar, A., Chinnaiyan, A. M., Nuñez, G., and McDonald, C. (2012) The nucleotide synthesis enzyme CAD inhibits NOD2 antibacterial function in human intestinal epithelial cells. *Gastroenterology* **142**, 1483–1492
- Lipinski, S., Grabe, N., Jacobs, G., Billmann-Born, S., Till, A., Häslér, R., Aden, K., Paulsen, M., Arlt, A., Kraemer, L., Hagemann, N., Erdmann, K. S., Schreiber, S., and Rosenstiel, P. (2012) RNAi screening identifies mediators of NOD2 signaling: implications for spatial specificity of MDP recognition. *Proc. Natl. Acad. Sci. U.S.A.* **109**, 21426–21431
- Warner, N., Burberry, A., Franchi, L., Kim, Y. G., McDonald, C., Sartor, M. A., and Nuñez, G. (2013) A genome-wide siRNA screen reveals positive and negative regulators of the NOD2 and NF- $\kappa$ B signaling pathways. *Sci. Signal.* **6**, rs3

## HSP70 Regulates the Stability of NOD2

28. Rossi, F. M., Guicherit, O. M., Spicher, A., Kringstein, A. M., Fatyol, K., Blakely, B. T., and Blau, H. M. (1998) Tetracycline-regulatable factors with distinct dimerization domains allow reversible growth inhibition by p16. *Nat. Genet.* **20**, 389–393
29. Onesto, C., Berra, E., Grépin, R., and Pagès, G. (2004) Poly(A)-binding protein-interacting protein 2, a strong regulator of vascular endothelial growth factor mRNA. *J. Biol. Chem.* **279**, 34217–34226
30. Meylan, E., Curran, J., Hofmann, K., Moradpour, D., Binder, M., Bartenschlager, R., and Tschopp, J. (2005) Cardif is an adaptor protein in the RIG-I antiviral pathway and is targeted by hepatitis C virus. *Nature* **437**, 1167–1172
31. De Felipe, P., and Izquierdo, M. (2000) Tricistronic and tetracistronic retroviral vectors for gene transfer. *Hum. Gene Ther.* **11**, 1921–1931
32. Springer, M. L., and Blau, H. M. (1997) High-efficiency retroviral infection of primary myoblasts. *Somat. Cell Mol. Genet.* **23**, 203–209
33. Hisamatsu, T., Suzuki, M., Reinecker, H. C., Nadeau, W. J., McCormick, B. A., and Podolsky, D. K. (2003) CARD15/NOD2 functions as an antibacterial factor in human intestinal epithelial cells. *Gastroenterology* **124**, 993–1000
34. Mohanan, V., Temburni, M. K., Kappes, J. C., and Galileo, D. S. (2013) L1CAM stimulates glioma cell motility and proliferation through the fibroblast growth factor receptor. *Clin. Exp. Metastasis* **30**, 507–520
35. Livak, K. J., and Schmittgen, T. D. (2001) Analysis of relative gene expression data using real-time quantitative PCR and the  $2(-\Delta\Delta C(T))$  method. *Methods* **25**, 402–408
36. Benabdellah, K., Cobo, M., Muñoz, P., Toscano, M. G., and Martin, F. (2011) Development of an all-in-one lentiviral vector system based on the original TetR for the easy generation of Tet-ON cell lines. *PLoS One* **6**, e23734
37. Zhao, L., Kwon, M. J., Huang, S., Lee, J. Y., Fukase, K., Inohara, N., and Hwang, D. H. (2007) Differential modulation of Nods signaling pathways by fatty acids in human colonic epithelial HCT116 cells. *J. Biol. Chem.* **282**, 11618–11628
38. Mayer, M. P., Brehmer, D., Gässler, C. S., and Bukau, B. (2001) HSP70 chaperone machines. *Adv. Protein Chem.* **59**, 1–44
39. Afrazi, A., Sodhi, C. P., Good, M., Jia, H., Siggers, R., Yazji, I., Ma, C., Neal, M. D., Prindle, T., Grant, Z. S., Branca, M. F., Ozolek, J., Chang, E. B., and Hackam, D. J. (2012) Intracellular heat shock protein-70 negatively regulates TLR4 signaling in the newborn intestinal epithelium. *J. Immunol.* **188**, 4543–4557
40. Van Molle, W., Wielockx, B., Mahieu, T., Takada, M., Taniguchi, T., Sekikawa, K., and Libert, C. (2002) HSP70 protects against TNF-induced lethal inflammatory shock. *Immunity* **16**, 685–695
41. Vinokurov, M., Ostrov, V., Yurinskaya, M., Garbuz, D., Murashev, A., Antonova, O., and Evgen'ev, M. (2012) Recombinant human HSP70 protects against lipoteichoic acid-induced inflammation manifestations at the cellular and organismal levels. *Cell Stress Chaperones* **17**, 89–101
42. Yokota, S., Kitahara, M., and Nagata, K. (2000) Benzylidene lactam compound, KNK437, a novel inhibitor of acquisition of thermotolerance and heat shock protein induction in human colon carcinoma cells. *Cancer Res.* **60**, 2942–2948
43. Schütze, S., Wiegmann, K., Machleidt, T., and Krönke, M. (1995) TNF-induced activation of NF- $\kappa$ B. *Immunobiology* **193**, 193–203
44. Beckmann, R. P., Mizzen, L. E., and Welch, W. J. (1990) Interaction of HSP70 with newly synthesized proteins: implications for protein folding and assembly. *Science* **248**, 850–854
45. Young, J. C., Agashe, V. R., Siegers, K., and Hartl, F. U. (2004) Pathways of chaperone-mediated protein folding in the cytosol. *Nat. Rev. Mol. Cell Biol.* **5**, 781–791
46. Schneider-Poetsch, T., Ju, J., Eyler, D. E., Dang, Y., Bhat, S., Merrick, W. C., Green, R., Shen, B., and Liu, J. O. (2010) Inhibition of eukaryotic translation elongation by cycloheximide and lactimidomycin. *Nat. Chem. Biol.* **6**, 209–217
47. Fava, F., and Danese, S. (2010) Crohn's disease: bacterial clearance in Crohn's disease pathogenesis. *Nat. Rev. Gastroenterol. Hepatol.* **7**, 126–128
48. Noguchi, E., Homma, Y., Kang, X., Netea, M. G., and Ma, X. (2009) A Crohn's disease-associated NOD2 mutation suppresses transcription of human IL10 by inhibiting activity of the nuclear ribonucleoprotein hnRNP-A1. *Nat. Immunol.* **10**, 471–479
49. Lee, K. H., Lee, C. T., Kim, Y. W., Han, S. K., Shim, Y. S., and Yoo, C. G. (2005) Heat shock protein 70 negatively regulates the heat-shock-induced suppression of the I $\kappa$ B/NF- $\kappa$ B cascade by facilitating I $\kappa$ B kinase renaturation and blocking its further denaturation. *Exp. Cell Res.* **307**, 276–284
50. Wiech, M., Olszewski, M. B., Tracz-Gaszewska, Z., Wawrzynow, B., Zylicz, M., and Zylicz, A. (2012) Molecular mechanism of mutant p53 stabilization: the role of HSP70 and MDM2. *PLoS One* **7**, e51426
51. Li, P., Ninomiya, H., Kurata, Y., Kato, M., Mياke, J., Yamamoto, Y., Igawa, O., Nakai, A., Higaki, K., Toyoda, F., Wu, J., Horie, M., Matsuura, H., Yoshida, A., Shirayoshi, Y., Hiraoka, M., and Hisatome, I. (2011) Reciprocal control of hERG stability by HSP70 and Hsc70 with implication for restoration of LQT2 mutant stability. *Circ. Res.* **108**, 458–468